ACS APPLIED MATERIALS & INTERFACES

www.acsami.org

Research Article

# Foams with Enhanced Rheology for Stopping Bleeding

Hema Choudhary,[†] Michael B. Rudy,[†] Matthew B. Dowling, and Srinivasa R. Raghavan*

Cite This: *ACS Appl. Mater. Interfaces* 2021, 13, 13958−13967

Read Online

ACCESS | Metrics & More | Article Recommendations | Supporting Information

**ABSTRACT:** Bleeding from injuries to the torso region is a leading cause of fatalities in the military and in young adults. Such bleeding cannot be stopped by applying direct pressure (compression) of a bandage. An alternative is to introduce a foam at the injury site, with the expansion of the foam counteracting the bleeding. Foams with an active hemostatic agent have been tested for this purpose, but the barrier created by these foams is generally not strong enough to resist blood flow. In this paper, we introduce a new class of foams with enhanced rheological properties that enable them to form a more effective barrier to blood loss. These aqueous foams are delivered out of a double-barrelled syringe by combining precursors that produce bubbles of gas ($CO_2$) *in situ*. In addition, one barrel contains a cationic polymer (hydrophobically modified chitosan, hmC) and the other an anionic polymer (hydrophobically modified alginate, hmA). Both these polymers function as hemostatic agents due to their ability to connect blood cells into networks. The amphiphilic nature of these polymers also enables them to stabilize gas bubbles without the need for additional surfactants. hmC−hmA foams have a mousse-like texture and exhibit a high modulus and yield stress. Their properties are attributed to the binding of hmC and hmA chains (*via* electrostatic and hydrophobic interactions) to form a coacervate around the gas bubbles. Rheological studies are used to contrast the improved rheology of hmC−hmA foams (where a coacervate arises) with those formed by hmC alone (where there is no such coacervate). Studies with animal wound models also confirm that the hmC−hmA foams are more effective at curtailing bleeding than the hmC foams due to their greater mechanical integrity.

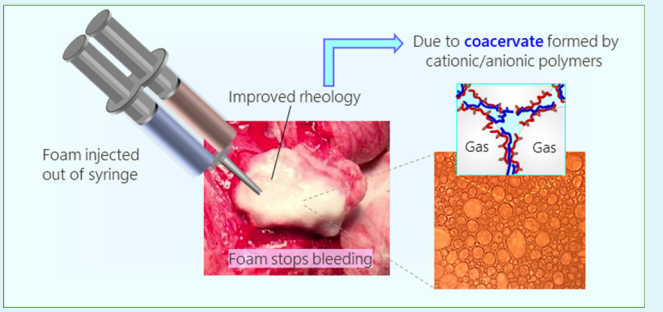


**KEYWORDS:** *foam rheology, foam formulation, associating polymer, complex coacervation, hemostatic biomaterial*



## INTRODUCTION

Liquid foams are colloidal dispersions of gas bubbles in a continuous liquid phase.[1−4] The bubbles in these foams are typically stabilized by surfactant molecules, which adsorb on the bubbles (i.e., at the gas−liquid interface) due to their amphiphilic character.[1] The surfactants orient their hydrophobic tails toward the gas and their hydrophilic heads toward the liquid phase; as a result, coalescence of bubbles is inhibited.[1,4] Foams stabilized by common surfactants like sodium dodecyl sulfate (SDS) typically remain stable only for a few minutes, however.[3] As time progresses, the liquid between adjacent bubbles drains away and the bubbles coarsen into larger structures until eventually the bubbles dissipate away.[1,3] To enhance the stability of foams, surfactants can be replaced by particles that adsorb irreversibly at the gas−liquid interface.[5,6] Such foams are termed Pickering foams in analogy with Pickering emulsions.[7] Instead of directly adding particles, another strategy is to generate the particles *in situ* by combining a surfactant like SDS and a salt like potassium chloride (KCl).[8] Foams are also frequently encountered in food science, and an alternative way to stabilize food-grade foams is by using amphiphilic proteins, either on their own or combined with polysaccharides.[9−11]

Our interest in foams stems from their use to treat bleeding. Uncontrolled bleeding (hemorrhage) is a leading cause of death for soldiers on the battlefield and for civilian young adults.[12−14] Among bleeding injuries, those to the trunk or torso region cannot be treated by applying direct compression of a bandage.[13,14] Such noncompressible injuries account for the majority of bleeding-related fatalities.[13,14] Recently, we described the use of foams based on hydrophobically modified chitosan (hmC) to treat such injuries.[15] Foams are attractive because an expanding foam at the injury site counteracts the discharge of blood without external compression.[16] Following expansion, the foam forms a barrier (due to its solid-like nature), allowing active ingredients ("hemostatic agents") in the foam to interact with and coagulate blood. We have previously shown that hmC acts as a hemostatic agent due to its ability to connect blood cells into a physical network.[17−19]

**Received:** January 4, 2021
**Accepted:** March 3, 2021
**Published:** March 22, 2021

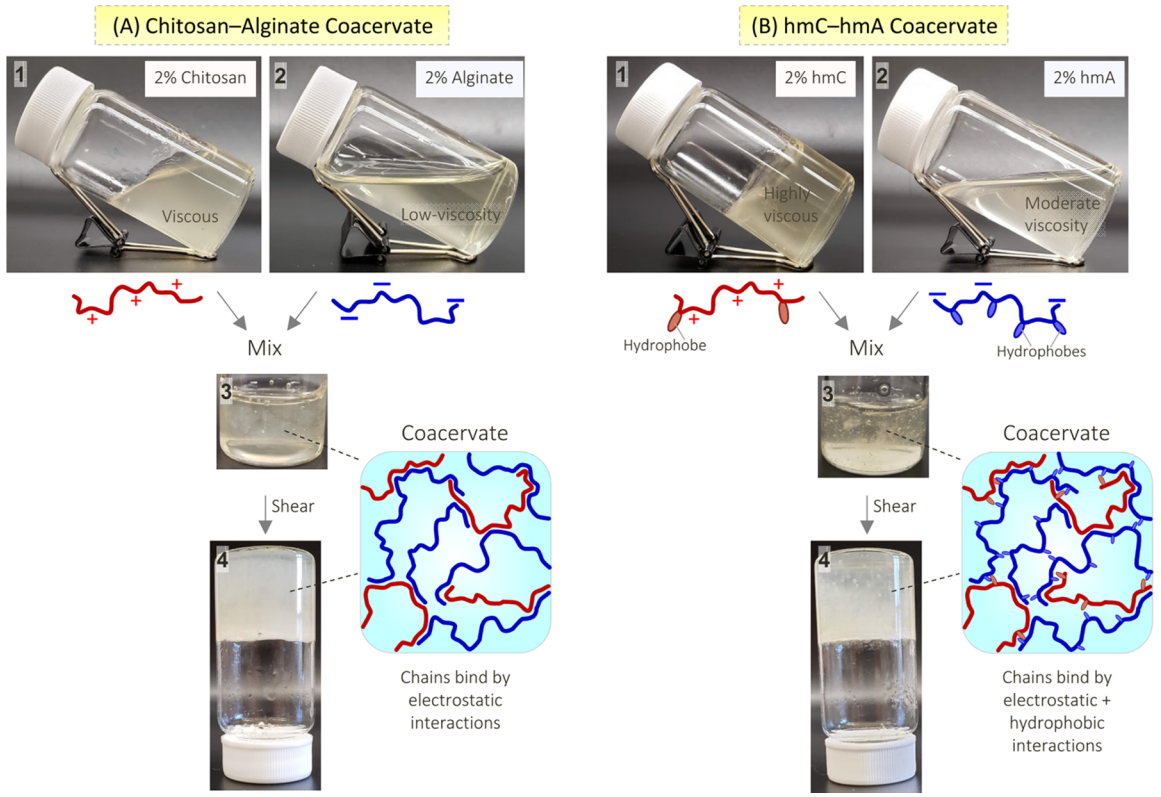


**Figure 1. Coacervate formation in chitosan–alginate and hmC–hmA mixtures.** (A) When solutions of 2% chitosan (1) and 2% alginate (2) are mixed, the mixture appears inhomogeneous (3), and upon vortex mixing, it becomes gel-like and retains its weight in the inverted vial (4). This is because the polymer chains form a coacervate, i.e., they bind by electrostatic interactions into a network, as shown by the inset schematic. (B) Similar coacervation is seen with mixtures of hydrophobically modified chitosan (hmC) and hydrophobically modified alginate (hmA). These polymers have alkyl tails along their backbone, and the ensuing hydrophobic interactions between the chains make their solutions viscous. When solutions of 2% hmC (1) and 2% hmA (2) are mixed, the mixture again shows inhomogeneities (3), and upon vortex mixing, it also becomes gel-like and holds its weight in the inverted vial (4). Here, the coacervate arises due to a combination of electrostatic and hydrophobic interactions between the polymer chains.

In addition, the amphiphilic hmC also stabilizes the bubbles in the foam—thus, the foam can be created without surfactants, which are undesirable in biomedical applications because surfactants tend to denature proteins and are often cytotoxic. Surfactant-free hemostatic foams based on hmC have been used to arrest bleeding from severe, lethal injuries in pigs and rats.[15,20,21]

In working with the above hemostatic foams, we have recognized the need for certain improvements in foam properties. Ideally, the foam should persist at the wound site for sufficient time to allow the active ingredient to interact with blood and stop its discharge. However, hmC foams tend to be mechanically weak and sometimes get pushed aside by flowing blood. To form a more robust barrier to blood flow, a foam with enhanced rheology and a more solid-like texture (consistency) is needed. In this regard, we looked for insights from studies on foam rheology. Most of these studies have been done by applied physicists, and they all correlate *physical* parameters such as the bubble size and volume fraction with the elastic modulus $G'$ and the yield stress $\sigma_y$ of the foam.[22−24] Generally, the smaller the average bubble size, the higher the $G'$ and $\sigma_y$. While the bubble size does depend on the amount of stabilizer added, it would be useful to also know the effects of *chemical* variables on foam rheology, specifically those relating to the *type* of stabilizer or the composition of the continuous phase (surrounding the bubbles). However, to our knowledge, there have been few systematic studies connecting chemical variables to the rheology of foams.[25−28]

In this paper, we describe a new class of hemostatic foams with improved rheology. We employ a double-barrelled syringe (DBS) to generate this foam *in situ*: one barrel contains acetic acid, while the other contains sodium bicarbonate. The acid and base react at the DBS tip to form carbon dioxide ($CO_2$) gas in the form of bubbles. These bubbles are stabilized by polymers present in both solutions: in the acidic solution, we include hmC, while in the basic solution, we introduce hydrophobically modified alginate (hmA). The hmA is synthesized by attaching hydrophobic tails to the backbone of the anionic polysaccharide, alginate.[18] While hmA is anionic unlike the cationic hmC, both these amphiphilic polymers are known to serve as hemostatic agents.[17,18] At the DBS tip, the hmC and hmA mix and form a *coacervate* via electrostatic and hydrophobic interactions. (The term *coacervate* refers to a distinct phase formed by liquid–liquid phase separation in mixtures of oppositely charged polymers or surfactants.[29−37] A coacervate formed by two polymers is referred to as a "complex" coacervate[29] or a "polyelectrolyte complex".[32]) We study the foams by optical microscopy and rheology under both compression and shear. The rheology of hmC–hmA foams is found to be enhanced when compared to control foams with a single polymer. The enhanced rheology allows the hmC–hmA foams to establish a more robust barrier to blood discharge at a wound site, as we will show by studies


https://doi.org/10.1021/acsami.0c22818
ACS Appl. Mater. Interfaces 2021, 13, 13958−13967

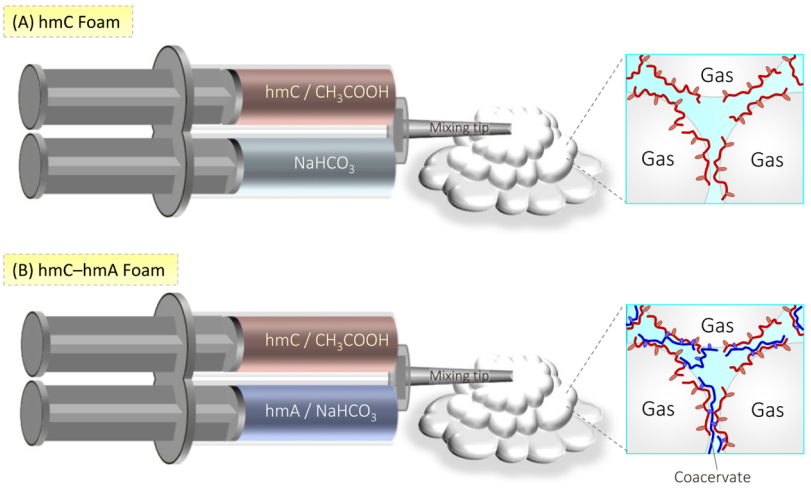


**Figure 2. Foam generation using a double-barrelled syringe (DBS).** (A) To generate an hmC foam, one barrel of the DBS has hmC dissolved in acetic acid ($CH_3COOH$) while the other barrel has a sodium bicarbonate ($NaHCO_3$) solution. At the mixing tip of the DBS, $CO_2$ gas is produced by the acid–base reaction, and bubbles of the gas are stabilized by hmC chains in the foam. (B) To generate an hmC–hmA foam, the same setup is employed but with the second barrel of the DBS containing hmA dissolved in $NaHCO_3$. In this case, the bubbles in the foam are stabilized by both hmC and hmA chains, which are collectively expected to form a coacervate.

with animal wound models. To our knowledge, surfactant-free foams stabilized by coacervates of oppositely charged polymers have never been studied before, and their remarkable properties should make them attractive for various applications.

## RESULTS AND DISCUSSION

**Coacervation.** First, we describe the phenomenon of coacervation in chitosan–alginate solutions. Figure 1A shows vials containing a 2% chitosan solution (in acetic acid) and a 2% alginate solution (in deionized or DI water). Chitosan has a p$K_a$ of 6.5 and thus in acidic media, its chains are cationic due to the protonation of amines along their backbone. Alginate chains, on the other hand, are anionic in solution due to the dissociation of their carboxylate groups. The chitosan used here has a high molecular weight, and a 2% solution of this chitosan is thereby quite viscous (photo 1). The 2% alginate solution is of a lower viscosity and flows readily in the tilted vial (photo 2). When the two solutions are gently mixed, discrete globs of a gooey material (the coacervate) are instantly formed, and these globs remain suspended in a clear external solution (photo 3). Upon shearing this sample using a vortex mixer, the globs are reduced in size and eventually, the entire sample appears near-homogeneous and turbid. The sample shows elastic or gel-like character, as reflected in its ability to hold its weight in the inverted vial (photo 4). Similar coacervation is known to occur with a variety of oppositely charged polymers.[31,37] The phenomenon occurs because the polymer chains bind to each other via electrostatic interactions and thereby neutralize their charges (see the schematic in Figure 1A). The binding of polymers results in counter ions being released, which increases the entropy of the system.[33] In the absence of a net charge, these "polyelectrolyte complexes" will be insoluble in water, and this explains their tendency to phase-separate.[29,35]

Similar phenomena are also observed in hmC–hmA solutions. The hmC studied here has hexadecyl ($C_{16}$) tails attached to 1.5% of the amines along the chitosan backbone.[17] The hydrophobes allow hmC chains to associate and thereby thicken the solution.[17,18] This is why a 2% hmC solution is extremely viscous or gel-like (Figure 1B, photo 1). In the case of the hmA, it has octyl ($C_8$) tails attached to 25% of the carboxylates along the alginate backbone.[18] Because the hydrophobes are shorter, the 2% hmA solution is only moderately viscous (photo 2 in Figure 1B). When the hmC and hmA solutions are mixed, the result is similar to that for chitosan–alginate: discrete globs of the coacervate appear (photo 3), and upon shearing, the globs are homogenized into a gel-like sample (photo 4). This coacervate gel is expected to contain a network of the hmC and hmA chains bound via both electrostatic and hydrophobic interactions (see the schematic in Figure 1B).[34] The gel-like behavior of these coacervates is also confirmed by dynamic rheology. Figure S1 (in the Supporting Information) shows plots of the elastic modulus $G'$ and the viscous modulus $G''$ as a function of frequency $\omega$. Both the chitosan-alginate coacervate (Figure S1a) and the hmC–hmA coacervate (Figure S1b) show gel-like rheology,[38,39] that is, $G' > G''$ across the $\omega$ range, and $G'$ approaches a plateau at low $\omega$. The plateau in $G'$ implies that the gel does not relax over long timescales.[38,39] The rheology also shows that the hmC–hmA coacervate is more elastic (higher ratio of $G'/G''$) and stiffer (higher value of $G'$) than the chitosan-alginate coacervate. Also, both coacervates have higher moduli compared to their parent polymer solutions.

**Foam Generation.** To generate the foams in our study, we use a DBS, as schematized in Figure 2. The foam is formed via the reaction of an acidic solution (acetic acid, $CH_3COOH$) and a basic solution (sodium bicarbonate, $NaHCO_3$) loaded in separate barrels of the DBS. The two solutions come into contact at the mixing tip, whereupon the following reaction occurs

$$CH_3COOH + NaHCO_3 \rightarrow CH_3COONa + CO_2(g) + H_2O \quad (1)$$

The net result is the formation of carbon dioxide ($CO_2$) gas in the form of bubbles. A foam arises instantly if these bubbles remain stable for some period of time, for which a stabilizer (e.g., a surfactant or an amphiphilic polymer) must be present in at least one of the barrels. In our case, we are interested in


https://doi.org/10.1021/acsami.0c22818
ACS Appl. Mater. Interfaces 2021, 13, 13958–13967

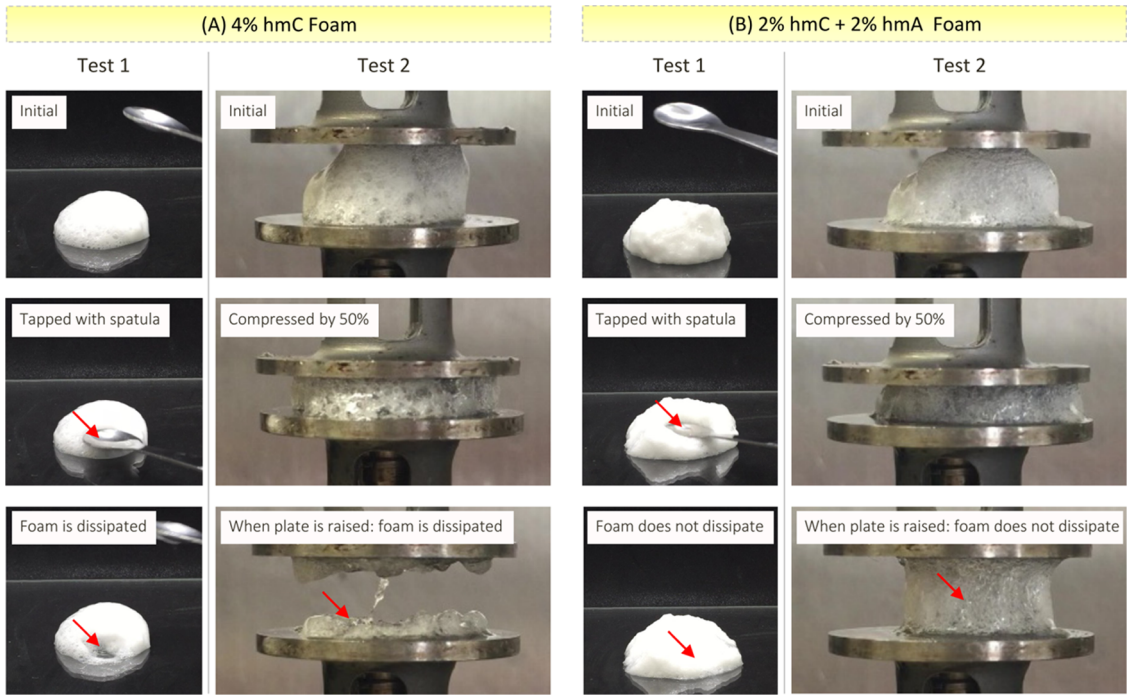


**Figure 3. Visual comparison of an hmC foam and an hmC−hmA foam.** Both have a total polymer concentration of 4 wt %. In Test 1, the foam is lightly tapped with a spatula. In Test 2, the foam is compressed between parallel plates to half of its initial height for 1 min, and then, the top plate is raised back. (A) With the hmC foam, in Test 1, the bubbles dissipate in the tapped area and the foam collapses. In Test 2, the compression causes the bubbles to burst and the foam is dissipated by the end. (B) With the hmC−hmA foam, in Test 1, the foam does not dissipate; rather it responds like an elastic object. In Test 2 also, the foam retains its integrity after the deformation.

surfactant-free foams due to their intended use in biomedical applications.[15] Therefore, an amphiphilic polymer (hmC or hmA or both) must be included for foam formation. If we only had the parent polymers (chitosan or alginate or both) in the DBS, we cannot form a stable foam.[15]

The key contrast in this work is between a foam made with hmC or hmA alone and one with *both* hmC and hmA. In the case of the hmC foam (Figure 2A), one barrel of the DBS has a solution of hmC in 1.1 M $CH_3COOH$, and the other has a solution of 1.1 M $NaHCO_3$. The bubbles in this foam will be stabilized by hmC chains, and there will be no coacervate. Note that the use of identical molarities for the acid and base ensures that the foam will have a near-neutral pH, which we confirmed via a pH sensor. In the case of the hmC−hmA foam (Figure 2B), the first barrel has the hmC solution as before, while the other barrel has a solution of hmA in the base. The bubbles in this foam will be stabilized by hmC and hmA chains that will collectively be in a coacervate (or, put differently, the coacervate will surround the bubbles). The question then is whether this coacervate will have a significant effect on the properties of the foam.

**Foam Appearance, Stability, and Microstructure.** First, we will use visual observations and optical microscopy to contrast an hmC−hmA foam and one with hmC. (The foams with hmC or hmA alone are similar in most respects, and so the contrast is made with the hmC one.) Figure 3A shows photos of a foam made with 4% hmC and Figure 3B has photos of a foam made with 2% hmC and 2% hmA. The concentrations were chosen such that the total polymer content in the two foams was the same. Both these foams expand when released out of the DBS tip, but they have different textures. With regard to foam stability, we studied this by injecting the above foams into vials and measuring the height of the foams as time progressed (Figure S2, Supporting Information). The hmC foam reduced appreciably in height within 30 min, with some of the dissipated foam remaining stuck to the vial walls. The hmC−hmA foam, on the other hand, remained stable for a much longer time and reduced to around half its height in ∼2 h. Thus, hmC−hmA mixtures impart greater stability to the foam compared to hmC alone.

We now focus on the mechanical (rheological) properties of the foams in their stable, expanded state. The foams have very different rheology, and this is reflected in the photos in Figure 3. Test 1 in Figure 3A,B compares the responses of the foams to a gentle perturbance from a spatula. When an area of the hmC foam is tapped by the spatula, the bubbles dissipate and the foam collapses over the disturbed area. This shows the fragility of the hmC foam. In contrast, when the hmC−hmA foam is tapped by the spatula, the foam deforms over the affected area, but it does not dissipate or collapse. Instead, this foam exhibits an elastic response—that is, it recoils against the applied deformation. Test 2 shows the differences between the foams in another way. Here, each foam is placed between parallel plates and the top plate is brought down to compress the foam. After compression to half its initial height for a minute, the top plate is retracted to its initial height. Figure 3A reveals that the compression causes most of the bubbles in the hmC foam to dissipate. When the plate is raised back, the residue from the foam remains adhered to each plate, but most of the bubbles in the middle have disappeared. This demonstrates the inability of the foam to withstand compressive stress. Conversely, the bubbles do not break in the hmC−hmA foam when the plates are compressed (Figure 3B). When the plate is raised back, the foam sticks to both plates but still retains its integrity. We can summarize the differences between the above foams by making analogies to


https://doi.org/10.1021/acsami.0c22818
ACS Appl. Mater. Interfaces 2021, 13, 13958−13967

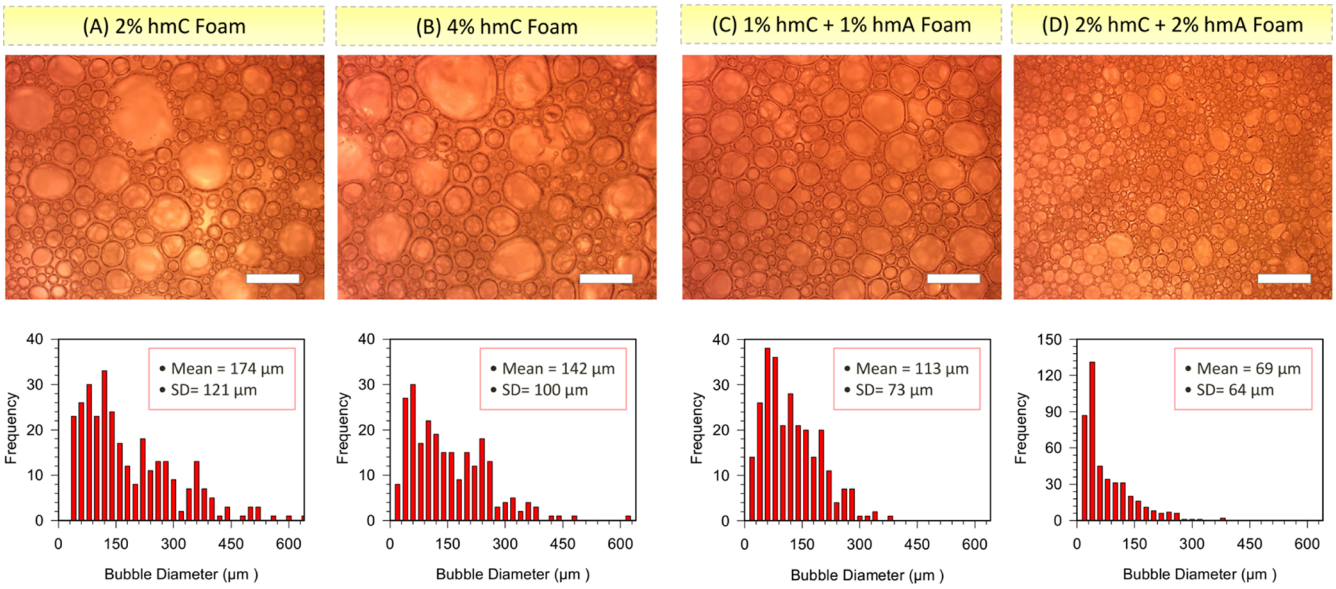


**Figure 4. Optical micrographs of foams with various polymer contents and the corresponding bubble size distributions:** (A) 2% hmC; (B) 4% hmC; (C) 1% hmC + 1% hmA; (D) 2% hmC + 2% hmA. Foams (A,C) have the same total polymer concentration as do foams (B,D). The corresponding bubble size distributions are shown as histograms and were obtained by analyzing several images of each foam. All scale bars are 750 $\mu$m.

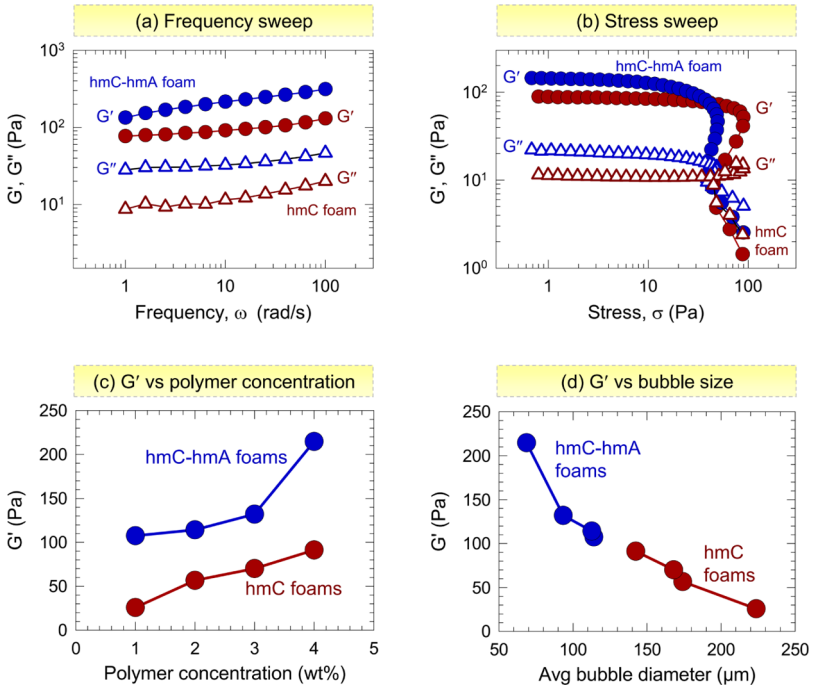


**Figure 5. Dynamic rheology of hmC and hmC−hmA foams.** In (a,b), data are compared for a 4% hmC foam and a 2% hmC + 2% hmA foam (same total polymer content). The data plotted are for the elastic modulus $G'$ (filled circles) and the viscous modulus $G''$ (unfilled triangles) as functions of (a) frequency and (b) stress amplitude at a constant frequency of 10 rad/s. In (c), $G'$ values for hmC and hmC−hmA foams are plotted against the total polymer concentration. In (d), the same $G'$ data are plotted against the average bubble diameter in the foams.

common foams: the texture or consistency of the hmC foam is similar to that of a frothy material such as a shower foam, whereas the hmC−hmA foam has a consistency comparable to that of a thick mousse or meringue.

Next, we characterized the hmC and hmC−hmA foams by optical microscopy. Representative images are provided for hmC foams (Figure 4A,B) and hmC−hmA foams (Figure 4C,D) at total polymer concentrations of 2 and 4%. In all cases, as expected, the images show numerous bubbles that fill up the entire view. The bubbles are not closely packed in the hmC foams (bubble volume fraction 50−60%), and one can see small gaps between them. The bubbles do appear nearly closely packed in the hmC−hmA foams (bubble volume fraction 60−70%), although Plateau borders are not seen between the bubbles (which would arise if the bubbles were tightly packed). Bubble sizes from these images were analyzed using ImageJ, and the distributions are provided for each sample. A striking observation is that the bubbles are smaller in


https://doi.org/10.1021/acsami.0c22818
ACS Appl. Mater. Interfaces 2021, 13, 13958−13967

the hmC−hmA foams than in the hmC foams. The mean diameter of the bubbles is calculated from each distribution and is provided below the images. This diameter is 174 and 142 $\mu$m for the 2 and 4% hmC foams, whereas it is 113 and 69 $\mu$m for the 2 and 4% hmC−hmA foams. Moreover, the distributions show that there are hardly any bubbles larger than 200 $\mu$m in the hmC−hmA foams, whereas the hmC foams have many such bubbles. Note also from the y-axes that there are far more bubbles in the hmC−hmA foams compared to the hmC ones.

**Foam Rheology.** We then proceeded to measure the rheological properties of hmC and hmC−hmA foams. First, we compared foams with 4% hmC and 2% hmC + 2% hmA using dynamic rheology (oscillatory shear). Figure 5a shows a plot of $G'$ and $G''$ as a function of $\omega$. Both foams show an elastic response, with $G' > G''$ and the moduli being nearly independent of frequency. The response indicates the solid-like behavior of the foams at low deformations (within the linear viscoelastic regime of the samples).[38,39] The key parameter from the plots is the elastic modulus $G'$, which is around 250 Pa for the hmC−hmA foam and 100 Pa for the hmC foam. Next, we kept the frequency constant at 10 rad/s and measured $G'$ and $G''$ against the stress amplitude $\sigma$ for both foams. Figure 5b shows that the moduli are independent of $\sigma$ at low stresses, and then, beyond a critical stress (i.e., the yield stress $\sigma_y$), the moduli rapidly decrease. From these plots, $\sigma_y$ is ∼50 Pa for both foams, i.e., there are no significant differences in this parameter between the two foams.

Additionally, we examined the variation of the foam modulus $G'$ with polymer concentration. We studied this for both the hmC and the hmC−hmA foams. The latter had equal concentrations of the two polymers—for example, a 2% foam corresponded to 1% hmC + 1% hmA. Dynamic rheology was performed on each sample and data for $G'$ at a frequency of 10 rad/s are plotted in Figure 5c. The results indicate that the hmC−hmA foams have higher $G'$ values across the concentration range. Note that $G'$ is a measure of the stiffness of the foam. Previous studies have correlated the foam modulus with the average bubble size and found that the smaller the bubbles, the higher the modulus of the foam.[22−24] Figure 5d shows plots of $G'$ against the average bubble diameter obtained from optical microscopy. This relationship is shown for both the hmC and the hmC−hmA foams. In both cases, $G'$ does increase as the bubbles get smaller. However, the two sets of foams do not overlap on this plot, indicating that the nature of the stabilizer (a single polymer vs a coacervate) does influence the foam rheology. Note that the bubble diameters are considerably smaller across the entire concentration range for the hmC−hmA foams compared to that for the hmC foams.

In the literature, foam rheology is often analyzed by normalizing the foam modulus $G'$ by the Laplace pressure ($\gamma/R$), where $\gamma$ is the surface tension and $R$ is the bubble radius.[24−26] This normalized modulus has been shown to be independent of the stabilizer type and concentration. For our data, a plot of $G'R/\gamma$ against polymer concentration is shown in Figure S3 (Supporting Information). To make this plot, we used typical values of the surface tension for hmC and hmA solutions from previous studies (in both cases, $\gamma \sim 35$ mN/m).[40,41] The hmC−hmA coacervate was also assumed to have the same $\gamma$ as coacervation should have no effect on $\gamma$.[36] The bubble radius $R$ for each foam was taken from Figure 5d. Figure S3 shows that the normalized modulus does not collapse into a single curve. On the contrary, the normalized moduli for the hmC−hmA foams are higher than those for the hmC foams. Thus, the data clearly show the effects of both the stabilizer type and concentration on foam rheology.

One question that is worth discussing is if the rheology is consistent with visual observations. The visual observations in Figure 3 indicated significant differences between the two kinds of foams. The rheology (Figure 5) does show that the hmC−hmA foams are stiffer (higher $G'$) than the hmC foams, but the difference is only a factor of 2.5 at best. Why is the difference not larger? One point to note is that these foams are mostly composed of gas (bubbles), and thus, the continuous (liquid) phase is a minor component in the foam. In fact, when the bubbles are closely packed, the continuous phase is almost nonexistent—the differences between the foams will then manifest only at the gas−liquid interface. If so, the impact of the combined hmC−hmA (and their resulting coacervate) will mainly be on bubble coalescence. Indeed, we saw in Figure 3 that bubbles did not coalesce when the hmC−hmA foam was compressed, whereas much more coalescence (and resulting foam dissipation) occurred when the hmC foam was compressed. The decreased bubble coalescence implies that hmC−hmA is a better stabilizer, and this is consistent with our earlier findings that hmC−hmA foams are stable for longer times (Figure S2).

Why does the coacervate inhibit bubble coalescence? There are several hypotheses to consider. First, bubbles in an hmC−hmA foam covered with a layer of coacervate might experience significant colloidal repulsions. In comparison, bubbles covered with hmC chains might have weaker repulsions, allowing them to coalesce more easily. Alternatively, the key could be how the liquid between the bubbles drains (which then promotes coalescence). The liquid (i.e., the continuous phase) between the bubbles could be appreciably increased in viscosity when hmC and hmA together form a coacervate. This thickening could impede liquid drainage and thereby inhibit coalescence. However, this second hypothesis cannot explain why a hmC foam with high polymer content (e.g., 4%) is still qualitatively different from a hmC−hmA foam with low polymer content (e.g., 1%). That is, simply increasing the hmC content (and thereby increasing the liquid viscosity) does not make its foam more like the hmC−hmA one. For this reason, we return to the first hypothesis that the coacervate indeed does contribute to greater repulsions between the bubbles. The coacervate may be forming a thicker and more robust layer around the bubbles compared to a single polymer. If so, when compressed the bubbles could deform but not burst, and when the compression is ceased, the deformed bubbles could revert to their original state. This would explain the elastic recoil observed in Figure 3B.

**Studies with Blood.** We now discuss the use of hmC−hmA foams as hemostatic materials, i.e., to stop bleeding. To examine this ability, we first conducted *in vitro* experiments with the foams in conjunction with blood. A simple tube-inversion test served as a preliminary indicator in this regard.[15] Here, 10 mL of heparinized bovine blood was first added to a 50 mL centrifuge tube. The foam (volume of 2 mL in each barrel of the DBS = 4 mL total) was injected into the tube from the nozzle of the DBS. The foam then expanded and filled the headspace in the tube. The tube was then inverted to see whether the foam could hold back the blood (Figure 6). In the case of the 4% hmC foam, the blood immediately flowed through the foam upon tube inversion (Figure 6A), indicating


https://doi.org/10.1021/acsami.0c22818
ACS Appl. Mater. Interfaces 2021, 13, 13958−13967

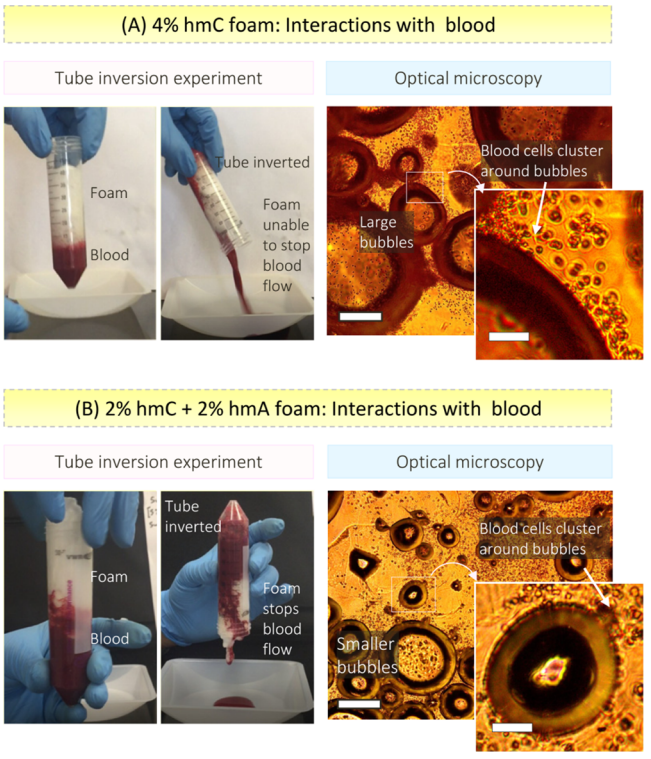


**Figure 6. Foam–blood interactions studied by a tube inversion test and by optical microscopy.** In the tube inversion test (left panel), the foam is introduced over bovine blood in a tube, and the tube is then inverted. The hmC foam (A) is unable to hold back the blood, whereas the hmC–hmA foam (B) is able to do so. In the bright-field optical micrographs (right panel), the blood cells are seen to cluster around the gas bubbles in both foams, which is due to the amphiphilic nature of hmC and hmA. The scale bars in the larger images correspond to 200 $\mu$m and in the smaller images to 40 $\mu$m.

that this foam does not constitute a sufficient mechanical barrier to blood flow. In contrast, the foam of 2% hmC + 2% hmA was able to hold back the blood in the inverted tube for several minutes (Figure 6B), confirming its higher mechanical integrity. Increasing the polymer concentration to 4% hmC + 4% hmA was enough to hold back the blood for over 20 min. We then doubled the amount of blood to 20 mL and repeated the test with this foam. The foam was able to hold back even this larger volume of blood for over 15 min. These results support the idea that hmC–hmA foams could be advantageous for hemostatic purposes.

To probe the interactions between the foams and blood, we also resorted to optical microscopy. From previous studies, we know that hmC and hmA can bind and connect blood cells through hydrophobic interactions.[17−19] In the case of a foam stabilized by one or both of these polymers, evidence for such interactions should arise around the gas bubbles. This was experimentally demonstrated in our previous study with hmC foams by bright-field microscopy,[15] and a similar procedure is adopted here. For these experiments, heparinized blood is diluted 10× in saline to ensure visibility of blood cells. The foams are mixed with this blood and then studied under bright-field microscopy. As expected, the images in Figure 6A (for an hmC foam) and in Figure 6B (for an hmC–hmA foam) both show blood cells clustering around the gas bubbles (note that there is also no hemolysis of the blood cells). Thus, the hm-polymers do behave as active hemostatic agents. However, for the polymers to interact with blood, sufficient contact time is needed. If the foam fails to provide a mechanical barrier, this contact time will be insufficient—and this is the case for the hmC foam (Figure 6A). Note also that in these *in vitro* experiments, clotting of blood *via* the usual clotting cascade has been eliminated by addition of heparin. In the case of *in vivo* experiments (see below), both the hm-polymers and the clotting cascade will act synergistically to immobilize the blood.

**Hemostatic Studies.** Encouraged by these results, we proceeded to test the hemostatic efficacy of hmC–hmA foams in pig liver-injury models. Initially, we compared a 2% hmC foam (sprayed out of a canister) and a 4% hmC + 4% hmA foam (injected out of a DBS) over an actively bleeding pig injury (Figure 7). Identical injuries were made using a 10 mm

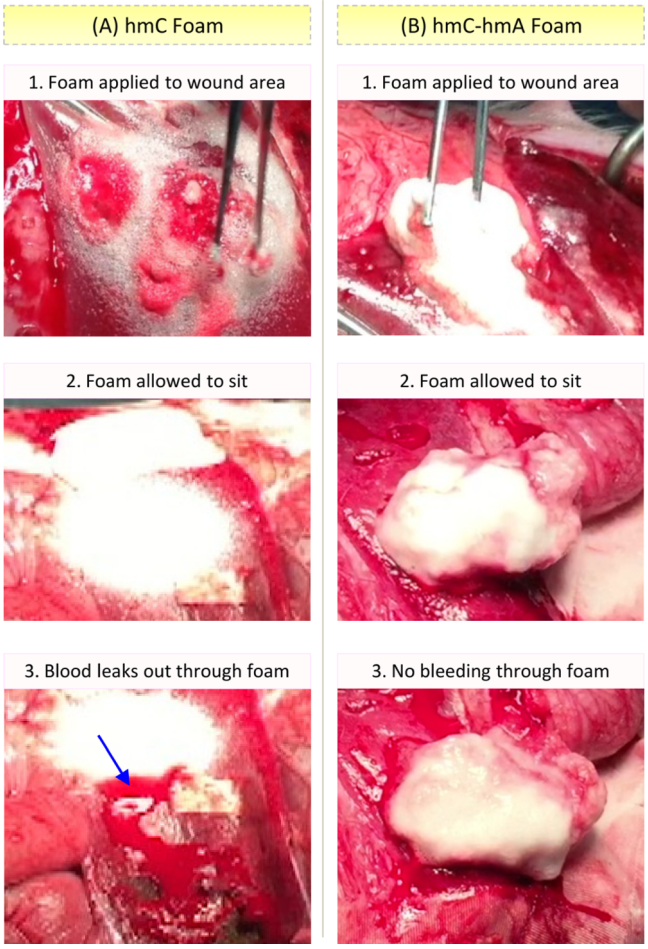


**Figure 7. Comparison of hmC and hmC–hmA foams as hemostatic agents over an actively bleeding pig liver injury.** (A) The 2% hmC foam is unable to contain the bleeding, and blood leaks through it. (B) The 4% hmC + 4% hmA foam remains an intact barrier to blood flow over the same time frame.

dermal punch and scissors, cutting a hole with a 10 mm diameter and a depth of several millimeters into the liver.[15] Thereafter, the foams were applied. We found that the hmC foam held back the blood initially, but after a few minutes, the blood seeped through, meaning that the foam was no longer effective at stopping the bleed (Figure 7A). In comparison, the hmC–hmA foam did not allow the blood to trickle through over the same time frame, and so the barrier due to the foam


https://doi.org/10.1021/acsami.0c22818
ACS Appl. Mater. Interfaces 2021, 13, 13958−13967

remained intact (Figure 7B). The results in Figure 7 confirm that the hmC−hmA foam establishes a more robust barrier to blood discharge due to its improved rheological properties. As noted above, once the foam impedes blood, it allows the blood to form a clot (gel) at the wound site, due to both interaction with hmC−hmA from the foam and the pig's own clotting cascade.

When testing both foams, we observed that the thinner hmC foam that was delivered out of the canister did have some attractive properties: it could quickly spread over a wide area and nicely wet the wound. This is a much-desired feature in an ideal hemostatic foam. In contrast, the thicker hmC−hmA foam could not fully cover and wet a large wound. This was partly because this foam was delivered out of a DBS, which is conducive to precise delivery at a point rather than coverage of a large area. It was also partly because of the mousse-like consistency of this foam, which meant that the foam remained as a lump on the surface rather than spreading out. These findings suggested that an optimal strategy could be to utilize both foams on the same injury to leverage their individual strengths. A test with both foams was therefore conducted (Figure 8). A liver injury was made as above with a 10 mm dermal punch. The hmC−hmA foam (4% of each polymer) was first applied, quickly followed by the 2% hmC foam. This combination allowed the hmC−hmA foam to serve as a robust barrier to the bulk of the blood flow, while the canister foam completely covered the wound and surrounding area. The foams were allowed to sit for over 5 min, during which no bleeding through the foams was observed. Then, the foams were removed, and even afterward, no additional bleeding occurred, indicating that hemostasis had been achieved (Figure 8). These results indicate that the combination of the two foams (hmC−hmA from the DBS and hmC alone from the canister) could be a viable strategy in the future to address large internal wounds. Further hemostatic tests will be needed to substantiate these preliminary results.

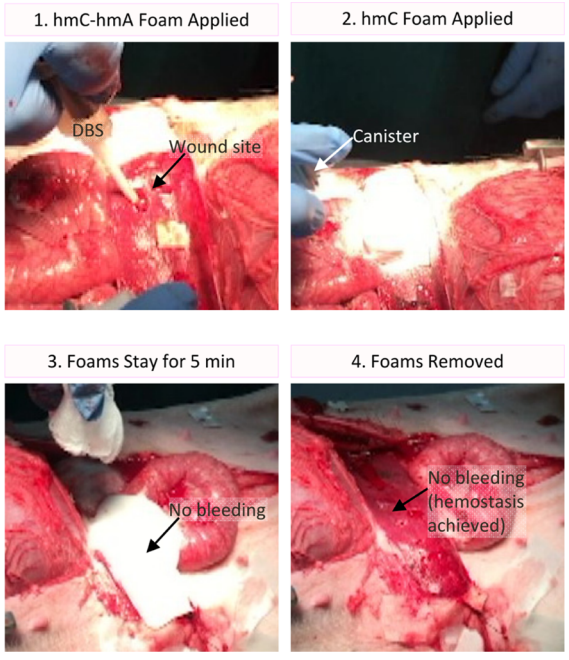


**Figure 8. Utilization of two foams concurrently on the same liver injury.** The 4% hmC + 4% hmA foam is first applied over the wound out of the DBS (1) and then the 2% hmC foam out of the canister (2). The combination proves successful in containing the bleeding (3), and hemostasis is achieved (4).

## CONCLUSIONS

In this paper, we prepared aqueous foams using two amphiphilic biopolymers—hmC (cationic) and hmA (anionic)—which are known for their hemostatic properties. A DBS was used to make the foams, with one barrel containing hmC in acid and the other hmA in base. The foam arose at the mixing tip of the DBS due to the $CO_2$ gas generated by the acid−base reaction. Bubbles of $CO_2$ were stabilized in the foam by hmC and hmA without the need for additional surfactants. Moreover, because of their opposite charge, hmC and hmA chains interacted strongly and formed a coacervate around the bubbles. We found that the rheological properties of hmC−hmA foams were enhanced compared to foams based on any one of the above polymers (hmC or hmA) alone. Visual tests showed that hmC−hmA foams had a mousse-like consistency and recoiled elastically when compressed. Rheological studies confirmed that hmC−hmA foams had higher elastic moduli compared to hmC foams. Microstructural characterization also revealed that the former had smaller bubbles and a greater density of the bubbles compared to the latter. Foams of hmC−hmA were tested for their ability to stop bleeding (achieve hemostasis) in pig-liver injury models. The mixed polymer foams were much better at curtailing bleeding than the hmC foams, i.e., they formed a more robust and impenetrable barrier to blood loss. Overall, hmC−hmA foams show promise for future applications as hemostatic agents. In addition, the strategy of using two oppositely charged polymers (and exploiting their coacervation) could be applied to foams in various other applications as well.

## EXPERIMENTAL SECTION

**Materials.** Chitosan (molecular weight 250−400 kDa, 99% deacetylated, product code 43020) was obtained from Primex Corp. (Iceland). Sodium alginate (product number A2033, sourced from brown algae, molecular weight of 80−120 kDa), *N*-(3-dimethylaminopropyl)-*N*-ethylcarbodiimide hydrochloride (EDC), *n*-octylamine (99%), hydrochloric acid (HCl), and sodium hydroxide (NaOH) were obtained from Sigma-Aldrich. Palmitic ($C_{16}$) anhydride (96.0%) and acetic acid ($CH_3COOH$) were obtained from TCI America. Arm & Hammer pure baking soda was the source of sodium bicarbonate ($NaHCO_3$). Bovine heparinized blood was sourced from Lampire Biological Products.

**Synthesis of hmC.** The following procedure, adapted from our previous work,[17−19] was used. First, 1 wt % chitosan was first dissolved in 0.2 M acetic acid. An equal volume of ethanol was then added, and the solution was heated to 65 °C. Palmitic anhydride was dissolved in a separate beaker with ethanol and heated to 65 °C. The anhydride solution was then added to the chitosan solution such that the stoichiometry corresponded to 1.5 mol % of the amines on the chitosan. The mixture was allowed to react overnight, whereupon the hmC was formed. To precipitate the hmC from this solution, the pH was raised by adding NaOH. The precipitate was then washed with ethanol several times, left to dry, and then ground into a powder. The resulting hmC will have $C_{16}$ hydrophobes with a degree of hydrophobe modification of 1.5%. That is, the reaction is expected to follow the stoichiometry, as verified in previous studies.[17,19] The hmC is soluble in water at acidic pH.

**Synthesis of hmA.** A procedure adapted from our previous work[18] was again used to synthesize the hmA. First, 2 wt % alginate was dissolved in water using HCl to make the solution acidic (with a pH of approximately 3.4). An aqueous solution of EDC (0.66 g/g of alginate) was then added to this solution, followed by the addition of


https://doi.org/10.1021/acsami.0c22818
ACS Appl. Mater. Interfaces 2021, 13, 13958−13967

*n*-octylamine (0.91 g/g of alginate) dissolved in 50/50 water/ethanol. The reaction was allowed to run for 24 h to form the hmA. The hmA was precipitated out by adding acetone into the reaction mixture. This precipitate was then washed several times with acetone and allowed to dry and then ground into a powder. The resulting hmA will have $C_8$ hydrophobes with a degree of hydrophobe modification of 25%; note that in this case, precise control of the modification degree is not possible.[18] Despite the high number of hydrophobes per chain, the hmA is water-soluble because the hydrophobes are short ($C_8$). If the hydrophobe length was $C_{10}$ or longer, the hmA would be insoluble in water. This is why we chose short hydrophobes on the hmA.[18]

**Double-Barreled Syringe Preparation.** The double-barreled syringes were obtained from J Dedoes, Inc. The dimensions of the barrel and plunger of the syringe were 3 mL × 3 mL. The mixing tip of the syringe was a 3 mm × 16 element blunt tip. The volume of solution loaded into each barrel was typically 2 mL. In one barrel, a solution of hmC (at a specific concentration) dissolved in 1.1 M $CH_3COOH$ was typically used. In the other barrel, the solution was either 1.1 M $NaHCO_3$ alone or with hmA dissolved in it at specific concentrations.

**Optical Microscopy.** In the case of the foams, a small amount of the foam was injected onto a glass slide and allowed to sit for a few minutes. Images were then captured on a Zeiss Axiovert 135 TV inverted microscope at 100× and 400× magnification. Bubble size distributions were analyzed using the ImageJ program. For each formulation, at least 10 images were analyzed. In the case of foam−blood mixtures, bovine heparinized blood was diluted 10× in saline and a drop of this was mixed with a small amount of the foam on a glass slide. A coverslip was then placed on the sample. Imaging was done at 100× magnification.

**Rheology.** All rheological experiments were performed using a TA Instruments AR2000 stress-controlled rheometer. Experiments were done at 25 °C using a parallel plate geometry (40 mm diameter). The surfaces of the plates had 24-grit sandpaper affixed to them. Dynamic frequency spectra were measured in the linear viscoelastic regime of the sample, which was evaluated by prior dynamic strain sweeps.

**Blood Experiments.** The DBS was loaded with 2 mL of solution in each barrel (4 mL total). Blood (10 or 20 mL) was added to a 50 mL centrifuge tube, and then, the foam was injected into the tube until it hit the surface of the blood. After the foam had expanded, the tube was inverted and held upside down to assess whether the foam could stop the blood flow due to gravity.

**Animal Studies.** Immature female Yorkshire swine (38 kg) were used in this study. The animals were housed in a climate-controlled facility consistent with protocols approved by the Association for Assessment and Accreditation of Laboratory Use Committee of Noble Life Sciences (Sykesville, MD). Food and water were available *ad libitum*. All animals received care in strict compliance with the National Research Council's Guide for Care and Use of Laboratory Animals. A liver injury, modeled after a standard parenchymal injury, was created by making multiple 10 mm (diameter) × 5 mm lesions using a sterile punch biopsy (Acu-Punch Biopsy Punch, Fisher Scientific). Biopsies were created in both the liver and spleen on an available surface, while the animal remained within 5% of the baseline mean arterial pressure (63 mm Hg). The biopsy punch injury denotes the start of the prehospital phase (time 0). After 30 s of free bleeding, the foam was applied to the biopsy site; 2 mL of the foam was applied to each biopsy site. The injury site was then observed for hemostasis: the achievement of hemostasis was defined as lack of visible bleeding through or around the edges of the foam after 2 min. The total observation time per experiment was 60 min. In cases where hemostasis was not achieved within the 2 min window, the bleed was stopped by cauterization. In this way, it was possible to make multiple injuries on one liver while still retaining the blood pressure of the pig to keep bleed rates consistent. For each type of sample, six experiments (replicates) were conducted.

## ■ ASSOCIATED CONTENT

### Supporting Information

The Supporting Information is available free of charge at https://pubs.acs.org/doi/10.1021/acsami.0c22818.

Dynamic rheology of coacervates, foam stability with time, and normalized modulus of foams as a function of the stabilizer concentration (PDF)

## ■ AUTHOR INFORMATION


### Corresponding Author

**Srinivasa R. Raghavan** − *Department of Chemical & Biomolecular Engineering, University of Maryland, College Park, Maryland 20742, United States;* orcid.org/0000-0003-0710-9845; Email: sraghava@umd.edu

### Authors

**Hema Choudhary** − *Department of Chemical & Biomolecular Engineering, University of Maryland, College Park, Maryland 20742, United States*

**Michael B. Rudy** − *Department of Chemical & Biomolecular Engineering, University of Maryland, College Park, Maryland 20742, United States*

**Matthew B. Dowling** − *Department of Chemical & Biomolecular Engineering, University of Maryland, College Park, Maryland 20742, United States*

Complete contact information is available at: https://pubs.acs.org/10.1021/acsami.0c22818

### Author Contributions

[†]H.C. and M.B.R. equal contribution.


### Notes

The authors declare the following competing financial interest(s): One of the authors (Matthew B. Dowling) is an employee of Medcura Inc, a company that is developing hemostatic products based on biopolymer derivatives.

## ■ ACKNOWLEDGMENTS

This work was partially supported by grants from the Maryland Industrial Partnerships (MIPS) program and from USAMRMC. We thank Dr. Joseph C. White for assistance with the preparation of the foams.

## ■ REFERENCES


(1) Weaire, D. L.; Hutzler, S. *The Physics of Foams*; Clarendon Press: Oxford; New York, 1999.

(2) Morrison, I. D.; Ross, S. *Colloidal Dispersions: Suspensions, Emulsions, and Foams*; Wiley-Interscience: New York, 2002.

(3) Pugh, R. J. Foaming, Foam Films, Antifoaming and Defoaming. *Adv. Colloid Interface Sci.* **1996**, *64*, 67−142.

(4) Durian, D. J.; Raghavan, S. R. Making a Frothy Shampoo or Beer. *Phys. Today* **2010**, *63*, 62−63.

(5) Hunter, T. N.; Pugh, R. J.; Franks, G. V.; Jameson, G. J. The Role of Particles in Stabilising Foams and Emulsions. *Adv. Colloid Interface Sci.* **2008**, *137*, 57−81.

(6) Dickinson, E. Food Emulsions and Foams: Stabilization by Particles. *Curr. Opin. Colloid Interface Sci.* **2010**, *15*, 40−49.

(7) Pickering, S. U. CXCVI.-Emulsions. *J. Chem. Soc. Trans.* **1907**, *91*, 2001−2021.

(8) Zhang, L.; Tian, L.; Du, H.; Rouzière, S.; Wang, N.; Salonen, A. Foams Stabilized by Surfactant Precipitates: Criteria for Ultrastability. *Langmuir* **2017**, *33*, 7305−7311.

(9) Narsimhan, G.; Xiang, N. Role of Proteins on Formation, Drainage, and Stability of Liquid Food Foams. *Annu. Rev. Food Sci. Technol.* **2018**, *9*, 45−63.
(10) Dickinson, E.; Izgi, E. Foam Stabilization by Protein-Polysaccharide Complexes. *Colloids Surf., A* **1996**, *113*, 191−201.
(11) Patino, J. M. R.; Pilosof, A. M. R. Protein-Polysaccharide Interactions at Fluid Interfaces. *Food Hydrocolloids* **2011**, *25*, 1925−1937.
(12) Kauvar, D. S.; Lefering, R.; Wade, C. E. Impact of Hemorrhage on Trauma Outcome: An Overview of Epidemiology, Clinical Presentations, and Therapeutic Considerations. *J. Trauma* **2006**, *60*, S3−S11.
(13) Martin, M.; Oh, J.; Currier, H.; Tai, N.; Beekley, A.; Eckert, M.; Holcomb, J. An Analysis of In-Hospital Deaths at a Modern Combat Support Hospital. *J. Trauma* **2009**, *66*, S51−S61.
(14) Kisat, M.; Morrison, J. J.; Hashmi, Z. G.; Efron, D. T.; Rasmussen, T. E.; Haider, A. H. Epidemiology and Outcomes of Non-Compressible Torso Hemorrhage. *J. Surg. Res.* **2013**, *184*, 414−421.
(15) Dowling, M. B.; MacIntire, I. C.; White, J. C.; Narayan, M.; Duggan, M. J.; King, D. R.; Raghavan, S. R. Sprayable Foams Based on an Amphiphilic Biopolymer for Control of Hemorrhage Without Compression. *ACS Biomater. Sci. Eng.* **2015**, *1*, 440−447.
(16) Holcomb, J. B.; McClain, J. M.; Pusateri, A. E.; Beall, D.; Macaitis, J. M.; Harris, R. A.; MacPhee, M. J.; Hess, J. R. Fibrin Sealant Foam Sprayed Directly on Liver Injuries Decreases Blood Loss in Resuscitated Rats. *J. Trauma* **2000**, *49*, 246−250.
(17) Dowling, M. B.; Kumar, R.; Keibler, M. A.; Hess, J. R.; Bochicchio, G. V.; Raghavan, S. R. A Self-Assembling Hydrophobically Modified Chitosan Capable of Reversible Hemostatic Action. *Biomaterials* **2011**, *32*, 3351−3357.
(18) Javvaji, V.; Dowling, M. B.; Oh, H.; White, I. M.; Raghavan, S. R. Reversible Gelation of Cells Using Self-Assembling Hydrophobically-Modified Biopolymers: Towards Self-Assembly of Tissue. *Biomater. Sci.* **2014**, *2*, 1016−1023.
(19) MacIntire, I. C.; Dowling, M. B.; Raghavan, S. R. How Do Amphiphilic Biopolymers Gel Blood? An Investigation Using Optical Microscopy. *Langmuir* **2020**, *36*, 8357−8366.
(20) Dowling, M. B.; Smith, W.; Balogh, P.; Duggan, M. J.; MacIntire, I. C.; Harris, E.; Mesar, T.; Raghavan, S. R.; King, D. R. Hydrophobically-Modified Chitosan Foam: Description and Hemostatic Efficacy. *J. Surg. Res.* **2015**, *193*, 316−323.
(21) Logun, M. T.; Dowling, M. B.; Raghavan, S. R.; Wallace, M. L.; Schmiedt, C.; Stice, S.; Karumbaiah, L. Expanding Hydrophobically Modified Chitosan Foam for Internal Surgical Hemostasis: Safety Evaluation in a Murine Model. *J. Surg. Res.* **2019**, *239*, 269−277.
(22) Khan, S. A.; Schnepper, C. A.; Armstrong, R. C. Foam Rheology: III. Measurement of Shear Flow Properties. *J. Rheol.* **1988**, *32*, 69−92.
(23) Höhler, R.; Cohen-Addad, S. Rheology of Liquid Foam. *J. Phys. Condens. Matter* **2005**, *17*, R1041−R1069.
(24) Weaire, D. The Rheology of Foam. *Curr. Opin. Colloid Interface Sci.* **2008**, *13*, 171−176.
(25) Marze, S. P. L.; Saint-Jalmes, A.; Langevin, D. Protein and Surfactant Foams: Linear Rheology and Dilatancy Effect. *Colloids Surf., A* **2005**, *263*, 121−128.
(26) Marze, S.; Guillermic, R. M.; Saint-Jalmes, A. Oscillatory Rheology of Aqueous Foams: Surfactant, Liquid Fraction, Experimental Protocol and Aging Effects. *Soft Matter* **2009**, *5*, 1937−1946.
(27) Denkov, N. D.; Tcholakova, S.; Golemanov, K.; Ananthpadmanabhan, K. P.; Lips, A. The Role of Surfactant Type and Bubble Surface Mobility in Foam Rheology. *Soft Matter* **2009**, *5*, 3389−3408.
(28) Engelhardt, K.; Lexis, M.; Gochev, G.; Konnerth, C.; Miller, R.; Willenbacher, N.; Peukert, W.; Braunschweig, B. pH Effects on the Molecular Structure of $\beta$-Lactoglobulin Modified Air-Water Interfaces and Its Impact on Foam Rheology. *Langmuir* **2013**, *29*, 11646−11655.
(29) Overbeek, J. T. G.; Voorn, M. J. Phase separation in polyelectrolyte solutions. Theory of complex coacervation. *J. Cell. Comp. Physiol.* **1957**, *49*, 7−26.
(30) Langevin, D. Complexation of oppositely charged polyelectrolytes and surfactants in aqueous solutions. A review. *Adv. Colloid Interface Sci.* **2009**, *147−148*, 170−177.
(31) Shchipunov, Y. A.; Postnova, I. V. Water-soluble Polyelectrolyte Complexes of Oppositely Charged Polysaccharides. *Compos. Interfac.* **2009**, *16*, 251−279.
(32) Gucht, J. v. d.; Spruijt, E.; Lemmers, M.; Cohen Stuart, M. A. Polyelectrolyte Complexes: Bulk Phases and Colloidal Systems. *J. Colloid Interface Sci.* **2011**, *361*, 407−422.
(33) Fu, J.; Schlenoff, J. B. Driving Forces for Oppositely Charged Polyion Association in Aqueous Solutions: Enthalpic, Entropic, but Not Electrostatic. *J. Am. Chem. Soc.* **2016**, *138*, 980−990.
(34) Thuresson, K.; Nilsson, S.; Lindman, B. Effect of Hydrophobic Modification on Phase Behavior and Rheology in Mixtures of Oppositely Charged Polyelectrolytes. *Langmuir* **1996**, *12*, 530−537.
(35) Mattison, K. W.; Wang, Y.; Grymonpré, K.; Dubin, P. L. Micro- and Macro-Phase Behavior in Protein-Polyelectrolyte Complexes. *Macromol. Symp.* **1999**, *140*, 53−76.
(36) Onesippe, C.; Lagerge, S. Study of the Complex Formation Between Sodium Dodecyl Sulfate and Hydrophobically Modified Chitosan. *Carbohydr. Polym.* **2008**, *74*, 648−658.
(37) Rabelo, R. S.; Tavares, G. M.; Prata, A. S.; Hubinger, M. D. Complexation of chitosan with gum Arabic, sodium alginate and $\kappa$-carrageenan: Effects of pH, polymer ratio and salt concentration. *Carbohydr. Polym.* **2019**, *223*, 115120.
(38) Macosko, C. W. *Rheology: Principles, Measurements, and Applications*; Wiley-VCH: New York, 1994.
(39) Larson, R. G. *The Structure and Rheology of Complex Fluids*; Oxford University Press: New York, 1999.
(40) Babak, V. G.; Desbrières, J. Dynamic Surface Tension of Hydrophobically Modified Chitosans. *Mendeleev Commun.* **2004**, *14*, 66−68.
(41) Wu, Z.; Wu, J.; Zhang, R.; Yuan, S.; Lu, Q.; Yu, Y. Colloid properties of hydrophobic modified alginate: Surface tension, $\zeta$-potential, viscosity and emulsification. *Carbohydr. Polym.* **2018**, *181*, 56−62.


https://doi.org/10.1021/acsami.0c22818
*ACS Appl. Mater. Interfaces* 2021, 13, 13958−13967

**Supporting Information for:**

# Foams with Enhanced Rheology for Stopping Bleeding

Hema Choudhary, Michael B. Rudy, Matthew B. Dowling and Srinivasa R. Raghavan*
Department of Chemical and Biomolecular Engineering, University of Maryland, College Park, MD 20742, USA
*Corresponding author. Email: sraghava@umd.edu

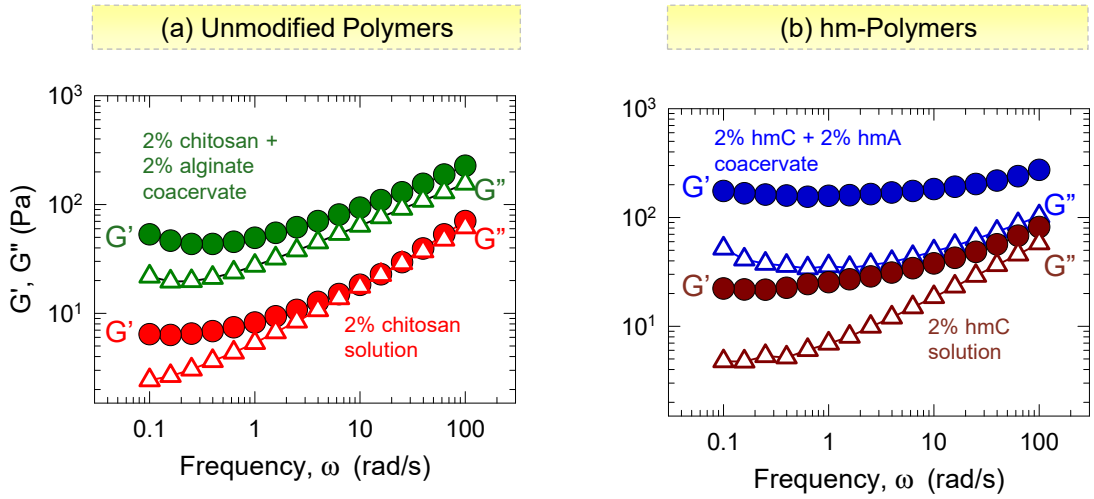


**Figure S1. Dynamic rheology of coacervates.** The elastic modulus $G'$ (filled circles) and the viscous modulus $G''$ (unfilled triangles) are plotted as functions of frequency. (A) Data for a chitosan-alginate coacervate and for the corresponding chitosan solution. (B) Data for a coacervate formed by hydrophobically modified chitosan (hmC) and hydrophobically modified alginate (hmA) and for the corresponding hmC solution. In all cases, the total polymer concentration is 2%.

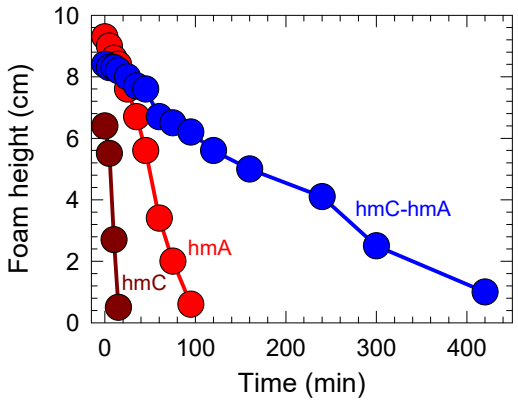


**Figure S2. Foam stability with time.** Each foam is injected into vials using double-barrelled syringes containing 1.5 mL in each barrel at time $t = 0$. The height of the foam as a function of time is measured and is shown in the above plot for foams made with: 4% hmA alone, 4% hmC alone, and 2% hmC + 2%hmA. The foam height decreases rapidly for the hmC and hmA foams compared to the hmC-hmA foam, indicating that the latter is more stable.

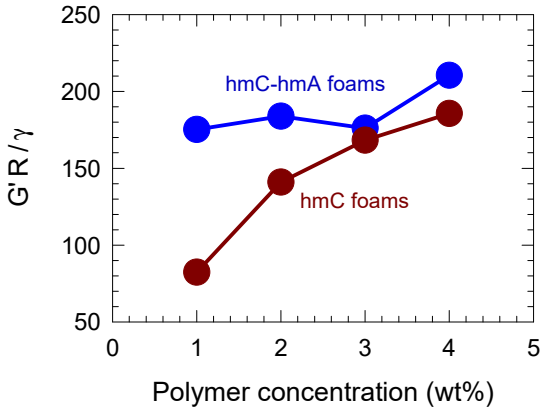


**Figure S3. Normalized modulus of foams as a function of the stabilizer concentration.** The elastic modulus $G'$ of hmC and hmC-hmA foams (data from Figure 5) is normalized by the Laplace pressure ($\gamma/R$) and plotted against the total polymer concentration in the foams. $\gamma$ is the surface tension and $R$ is the average radius of bubbles in the foam (data from Figure 5). The results for hmC-hmA foams fall above those for hmC foams, i.e., the results do not collapse onto a single master curve. This indicates that the *type* of polymeric stabilizer impacts the foam properties.